

The influence of shading control strategies on the visual comfort and energy demand of office buildings



Gyeong Yun, Kap Chun Yoon, Kang Soo Kim *

Department of Architecture, Korea University, 5-1 Anam-dong, Seongbuk-gu, Seoul 136-713, South Korea

ARTICLE INFO

Article history:

Received 28 April 2014

Received in revised form 19 June 2014

Accepted 20 July 2014

Available online 29 July 2014

Keywords:

Shading control strategy

Visual comfort

Energy demand

Venetian blind

EnergyPlus

ABSTRACT

A lighting control strategy using daylighting is important to reduce energy consumption, and to provide occupants with visual comfort. The objective of this research is to evaluate visual comfort and building energy demand, and suggest lighting and shading control strategies for visual comfort and building energy savings. This research intends to achieve visual comfort and energy savings in an office building, by means of visual environmental control, and focuses on a quantitative criterion (illuminance), and a qualitative criterion (glare index) in daylighting. We used HDR images captured in real scene and simulation (*DIVA-for-Rhino*) for glare evaluation. The measured data from the mock-up room and the scale model were compared, to validate the simulation tool. Vertical eye illuminance (E_v) is recommended for the glare index, in place of the DGI or DGP. To prevent disturbing glare and to secure maximum daylight, control strategies of lighting and shading are suggested, related to the E_v value. In addition, the *Energy-Plus* program was used for calculation of the annual energy consumption. Building energy consumption is presented according to three building orientations, and 10 control strategies of lighting and shading. If there is no need to consider glare, a blind slat angle of 0° or dynamic shading is better in winter, regardless of the building orientation. In summer, a blind slat angle of 30° (static angle) or dynamic shading is suitable for an energy efficient and anti-glare control strategy.

© 2014 Elsevier B.V. All rights reserved.

1. Introduction

Buildings account for approximately 40% of the world's annual energy consumption [1]. Building energy consumption is closely related to the lighting environment, according to daylighting. Daylighting is an important factor in determining indoor visual comfort, and affects user satisfaction and productivity [2]. In addition, daylighting from windows can bring both positive and negative experience: access to view and daylight, but also glare and thermal discomfort [3–5]. Occupants use personal computers; therefore, the issue of visual comfort comes to the fore as an essential element, particularly in office buildings. Daylighting has quite a different influence on the cooling, as against the heating load. In the cooling period, daylight negatively affects the cooling load; but the complete exclusion of daylight increases electric lighting energy consumption. In the heating period, daylight has a positive influence on the heating load, but an excessive amount of daylight affects discomfort glare.

Energy performance and the indoor environment have become increasingly important in building design [6]. In office buildings, the use of glass for façade designs has increased in recent years for aesthetic reasons, and this has caused excessive energy consumption, and glare. Daylighting is an effective and sustainable development strategy for enhancing visual comfort, energy-efficiency, and green building development [7]. Therefore, it is necessary to study the relationship between the visual environment and energy savings, according to the control strategy of electric lighting and daylighting.

Electric lighting is one of the major energy consuming items, and accounts for 20–30% of the total electric energy consumption [8]. In South Korea, lighting energy consumption comprises about 30% of the total building energy consumption [9]. Therefore, we should utilize daylighting for the cost-effective management of electric lighting.

A lighting control strategy using daylighting has been proposed, in order to reduce the energy consumption of new buildings or existing buildings. In addition to energy saving, the control strategy achieves visual comfort for the occupants.

The main objective of this study is to evaluate visual comfort and building energy demand, and suggest lighting and shading control strategies for visual comfort and building energy savings. This research intends to achieve visual comfort and energy savings, by

* Corresponding author. Tel.: +82 2 3290 3744; fax: +82 2 921 7947.

E-mail addresses: poprin@korea.ac.kr (G. Yun), kapchun@korea.ac.kr (K.C. Yoon), kskim@korea.ac.kr (K.S. Kim).

visual environmental control in an office building, and focuses on quantitative criteria (as illuminance), and qualitative criteria (as glare index), in daylighting.

The research is conducted for

- (1) the indoor environment of an office building,
- (2) the application of venetian blinds,
- (3) Seoul, Korea,
- (4) the climate condition of a whole year,
- (5) three orientations: south, east and west, and
- (6) during the weekday times of: 9:00 am to 6:00 pm.

2. Theory

2.1. Simulation programs

2.1.1. EnergyPlus

The *EnergyPlus* program is based on a combination of BLAST [10] and DOE-2 [11]. This program calculates with the heat balance of BLAST. The *EnergyPlus* daylighting algorithm is derived from the daylighting calculation in DOE-2.1E [12], which is described in Winkelmann [13], and Selkowitz [14]. In this research, we used the *EnergyPlus* program to predict the electric lighting energy and HVAC energy.

2.1.2. DIVA-for-Rhino

DIVA-for-Rhino is a daylighting and energy modeling plug-in for Rhinoceros. The plug-in was developed by the Graduate School of Design at Harvard University, and it is now developed by Solemma LLC [15]. *DIVA-for-Rhino* allows users to evaluate the environmental performance of buildings or urban landscapes. We can obtain radiation maps, photorealistic renderings, climate-based daylighting metrics, annual and individual time step glare analysis, LEED and CHPS daylighting compliance, and single thermal zone energy and load calculations.

Evalglare is applied to *DIVA-for-Rhino* in individual time step glare analysis, and we can obtain the HDR images for a specific point in time. The images were compared to the measured HDR images, for glare analysis, and vertical eye illuminance evaluation.

2.2. Glare indices

2.2.1. Daylight glare index (DGI)

Daylight glare index (DGI) predicts glare from a large source, such as a window. The BRE and Cornell University conducted this study [16]. The equation is expressed as follows.

$$DGI = 10 \log_{10} 0.48 \sum_{i=1}^n \frac{L_s^{1.6} \Omega_s^{0.8}}{L_b + 0.07 \omega_s^{0.5} L_s}$$

where L_s [cd/m^2] is the luminance of a glare source, L_b [cd/m^2] is the background luminance, ω_s [sr] is the solid angle subtended by the source, and Ω_s [sr] = ω_s/P is the solid angle subtended of the source, modified for the effect of the position of its elements in different parts of the field of view. The DGI criterion corresponding to the mean relation is as shown in Table 1.

2.2.2. Discomfort glare probability (DGP)

DGP is a glare index for the measurement of glare caused by daylight. The equation is defined as follows.

$$DGP = 5.87 \times 10^{-5} E_v + 9.18 \times 10^{-2} \log \left(1 + \sum_i \frac{L_{s,i}^2 \omega_{s,i}}{E_v^{1.87} P_i^2} \right) + 0.16$$

E_v [lx] is the vertical eye illuminance at eye level. DGP describes the fraction of disturbed occupants under the specific daylight

Table 1
Glare rating of DGI [17].

Glare criterion corresponding to mean relation	DGI
Just imperceptible	16
Noticeable	18
Just acceptable	20
Acceptable	22
Just uncomfortable	24
Uncomfortable	26
Just intolerable	28
Intolerable	30

situation. This index is developed by Wienold et al. [18]. The higher the DGP, the higher the glare.

The DGP criterion corresponding to the mean relation is as shown in Table 2.

In the Radiance tool called *evalglare*, DGP is based on the evaluation of the full luminance distribution of a visual field. This method is not convenient for a dynamic simulation, because it demands a picture for each time. Therefore, DGPs was generated, to be used in dynamic simulation by Daysim and *DIVA-for-Rhino*.

2.2.3. Simplified discomfort glare probability (DGPs)

DGPs was developed to overcome time-consuming repetitive work. Wienold and Christoffersen [17] revealed that the DGP and the vertical illuminance at eye level are interrelated. The equation is as follows.

$$DGPs = 6.22 \times 10^{-5} \times E_v + 0.184$$

In DGPs (simplified discomfort glare probability) calculation, the influence of glare sources is neglected. Therefore, this method should not be applied, when there is direct sun or specular reflection [20].

2.3. High dynamic range imaging

Humans can see objects in moonless night or bright sunny day. This means that the human eye can adapt to a dynamic luminance range of 10,000:1 [cd/m^2]. Most displays cannot present a dark area and a bright area in the same scene. A good quality LCD display has a dynamic range of about 1000:1.

High dynamic range imaging is a method to capture a higher dynamic range between the brightest and the darkest areas of an image, than those obtained by standard digital imaging methods. In general, non-HDR cameras take pictures with limited contrast range (known as low dynamic range (LDR) images), and one exposure at once. Therefore, we can only obtain images that do not show the darkest and the brightest details.

2.4. Evalglare

The *Evalglare* program was developed by Jan Wienold at the Fraunhofer Institute for Solar Energy Systems in Freiburg, Germany. This program evaluates the glare sources with 180° fish-eye images of Radiance image format, such as .pic or .hdr. For performance reasons, the image should be smaller than 800 × 800 pixel. The program calculates the glare indices (DGI, UGR VCP, and CGI) including

Table 2
Glare rating of DGP [19].

Glare rating	DGP
Imperceptible	<0.35
Perceptible	0.35–0.40
Disturbing	0.40–0.45
Intolerable	>0.45

Table 3

Recommended levels of illuminance.

Activity	IESNA		KS A 3011	
	Category	Illuminance [lx]	Category	Illuminance [lx]
Visual task of high contrast and large size	D	300	F	150–200–300
Visual task of medium contrast and small size	E	500	G	300–400–600
Visual task of high contrast and small size, or low contrast and large size	F	1000	H	600–1000–1500

the daylight glare probability (DGP), as basic output. Therefore, we can figure out the visual comfort with different indices.

Evalglare has many options to use for glare calculation. These are as follows [21].

- c: writing checkfile in Radiance picture format, for checking glare source.
- d: option for detailed output.
- vtt: setting the view type of picture file .vta for fisheye view
- vv: setting the view vertical size
- vh: setting the view horizontal size

If we use these options, all of information found from glare sources is printed as a glare file, and the last line indicates the following values:

1. DGP, 2. Average luminance of image, 3. Vertical eye illuminance, 4. Background luminance, 5. Direct vertical eye illuminance, 6. DGI, 7. UGR, 8. VCP, 9. CGI, 10. Average luminance of all glare sources, 11. Sum of solid angles of all glare sources, 12. Veiling luminance (disability glare), 13. X-direction of glare source, 14. Y-direction of glare source, 15. Z-direction of glare source.

The usage of the *evalglare* in this research is as follows: evalglare –c checkfile –vta –vv vertangle –vh horizangle –d hdrfile > glrfile

We can get the checkfile as .pic, and the glare file as .glr, for results.

2.5. Illuminance level

The Illuminating Engineering Society of North America (IESNA) publishes recommended design illuminance levels at the work plane, according to the task, background reflectance, visual acuity, required accuracy, and occupant age [22]. The Korean Standards Association (KSA) recommends the illuminance levels, according to the activities and uses of spaces (see Table 3) [23].

The three illuminance levels mean the minimum, the average, and the maximum values. For the same activity in office space, the IESNA and the KSA recommended a slightly different illuminance level. The Chartered Institution of Building Services Engineers (UK CIBSE Code) recommends the interior lighting level of 500 lx for general offices. In this research, we set the target illuminance to 500 lx, because electric lights are usually designed to satisfy this illuminance level at the work plane.

3. Methodology and measurements

3.1. Measurement of solar irradiances

The global horizontal irradiance and the diffuse irradiance are measured for the weather file. We use a pyranometer with shadow ring for the measurement, and this method requires some correction. The shadow ring of a pyranometer screens a portion of the sky, thus the measured diffuse irradiance must be corrected for the portion of the sky obscured by the shadow ring. There are many correction methods by Drummond [24], LeBaron et al. [25], Battles et al. [26] and Muneer and Zhang [27]. We used Muneer's anisotropic model for correction of the shadow ring, according to

our previous research [9]. We corrected the measured horizontal diffuse irradiance, and it is increased by 2–3%.

3.2. Mock-up room

A mock-up room represents a cell type office in the Korea University Daylighting Laboratory. An illuminance sensor was placed 1 m away from the window for the vertical eye illuminance measurement.

The mock-up room has a double-skin façade, and the outer window has a WWR of 100% and the inner window has a WWR of 71%. The reflectance of the inner surfaces is indicated in Table 5, the outer window transmittance and the inner window transmittance are 71% and 78%, respectively.

As shown in Fig. 1, an illuminance meter and a DSLR camera were set (see Table 4) to measure the vertical eye illuminance (E_v) and to take pictures for glare evaluation. Pyranometers (LP-PYRA 12, 02) measure the global horizontal irradiance [W/m^2] and the diffuse horizontal irradiance [W/m^2] to make the weather file for dynamic simulation. The data logger (Datascan 3000) transfers the stored data to the lab computer.

3.3. Equipment and software for glare evaluation

In the case of remodeling an existing building, the evaluation method for the present status of the visual environment is simple. We can use HDR images (HDRI) and the *evalglare* program to realize the present situation.

HDR images are used in *evalglare* for glare evaluation, and the AEB (Auto exposure bracketing) function of a DSLR camera with fisheye lens can be used. Two illuminance meters were attached to the fisheye lens, for the measurement of vertical illuminance (E_v) at eye level, to avoid the shadow from the window frame. This value was compared to E_v , from the output of *evalglare* with HDRI. E_v is related to the glare index such as DGP and DGPs.

There are many simulation tools for daylighting. The *Daysim* program can calculate the annual daylight availability, useful daylight illuminance, and DGPs (simplified discomfort glare probability), but one's visual field of a specified location cannot be derived from that tool, so we cannot obtain variable glare indices. Radiance and DIVA-for-Rhino can calculate the illuminance at any position and direction. In addition, we can obtain the HDR images from DIVA-for-Rhino simulation. Therefore, the authors compared the vertical eye illuminances measured with a mock-up room and scale model, to the derived results of *evalglare* with HDR images. The authors

Table 4

Cannon EOS 5D Mark II settings.

Feature	Setting
White balance	Daylight
Auto bracketing	On
Image size	S (2784 × 1856 pixels)
Sensitivity	ISO 100
Lens	Sigma F3.5 EX DG Fisheye Lens (180° field of view)
Luminance meter	Minolta LS-110 (1/3° field of view)
Illuminance meter	Minolta T-10

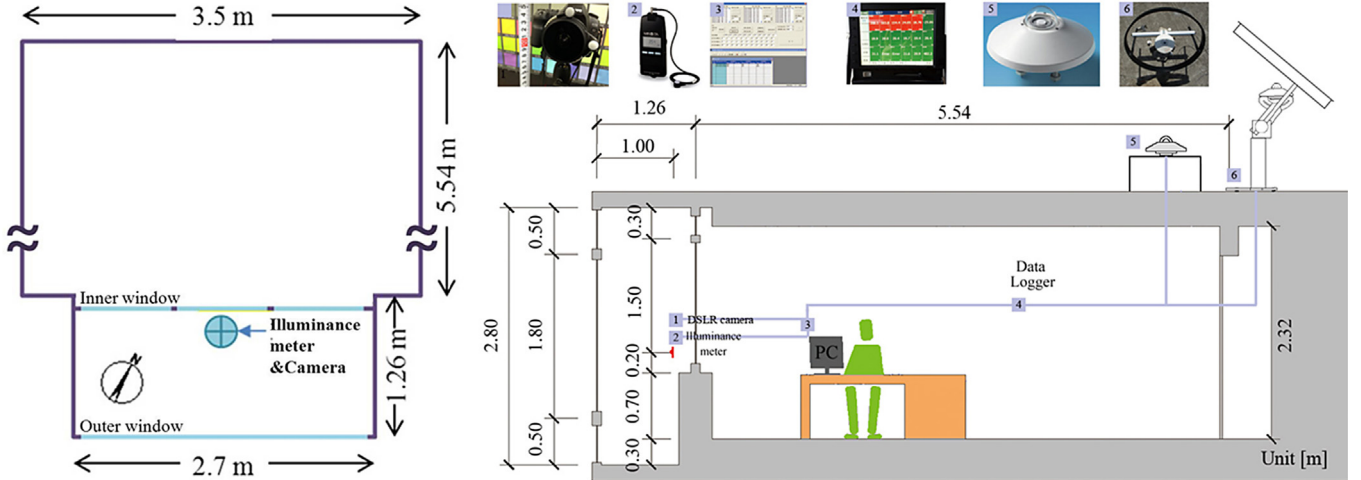


Fig. 1. Plan and section layout of the mock-up room.

also compared the DIVA-for-Rhino daylighting results to measured E_v and DGPs, in Section 4.1.

In order to obtain high dynamic range images, multiple exposure of the same scene must be taken, and combined using appropriate software. In this research, the Photosphere program [28] was used to make HDR images.

The three pictures were taken by the auto exposure bracketing (AEB) function of a DSLR camera. This function automatically changes the shutter speed or aperture, so that the exposure splits into three values, in the range of -2 to $+2$. In this research, fixed aperture size at $f/4.0$ and various shutter speeds were used in the manual exposure mode [29].

Photosphere is a photo-editing tool that allows to images to be edited, and HDR images to be easily made. When HDR images are made using Photosphere, cameras must be calibrated to obtain the correct images with a luminance meter (Minolta luminance meter LS-110 was used in this research). The digitally captured luminance of HDRI (High Dynamic Range Image) was matched to the real scene by this processing.

Photosphere supports several formats of output images, such as Radiance RGBE (HDR), TIFF, openEXR, and JPEG. The HDRI obtained from Photosphere was saved as Radiance RGBE format (.hdr), for glare evaluation by evalglare.

3.4. The integrated simulation method (ISM)

The electric lighting energy consumption is derived from importing the DIVA-for-Rhino lighting schedule (intgain.csv file) into the EnergyPlus lighting schedule. This ISM can predict the electric lighting energy consumption more accurately in the EnergyPlus program, and this affects the building total energy consumption calculation.

3.5. Simulation layout of DIVA-for-Rhino and EnergyPlus

In this research, DIVA-for-Rhino program was used to evaluate the annual glare (DGP) and vertical eye illuminance (E_v). The EnergyPlus program was used to evaluate the annual energy consumption, with the control strategy of lighting and shading. The test-space is shown in Fig. 2.

The orientation of the test space was south, east and west; the size was $5 \times 5 \times 3$ [m^3], and the reflectance of the inner surface was the same as that of the mock-up room. The window-wall-ratio (WWR) was 50%, and the location of the window was in the center

of the front wall of the building. Venetian blinds were installed on the outside of the window, and their specification is shown in Table 5. Most occupants do not frequently control the blinds; therefore the blind slat angles were determined by three angles: 0° , 15° and 30° .

The fraction radiant of the internal gains (people, lights and equipment) is referred to the 2009 ASHRAE HANDBOOK Fundamentals [30].

In DIVA-for-Rhino, a node is needed, to sense the threshold illuminance for shading control. In this study, an exterior node was selected for dynamic shading control.

DIVA-for-Rhino provides the advanced shading mode as climate-based metrics. We allow some layers to be controlled automatically, according to the illuminance at the selected nodes. DIVA-for-Rhino changes the layer according to the user's threshold illuminance setting. The test space has four layers—those of no shading, and slat angles of 0° , 15° , and 30° ; and the threshold values are set to control these layers. In most cases, automatic shading devices, or the lights, are controlled by an interior/exterior sensor on the ceiling, or exterior vertical wall. When the illuminance at the sensor rises beyond the specified threshold, the system automatically adjusts the shading system to the next lower setting (Base > State 1 > State 2 > State 3). On the other hand, once the illuminance threshold falls below a second user specified illuminance threshold, the system switches to the next higher state (State 3 > State 2 > State 1 > Base) [15].

We performed correlation between the $E_{v\text{out}}$ (exterior vertical illuminance) and $E_{v\text{in_1m}}$ (vertical eye illuminance) of 3000 lx, to find the threshold values in Fig. 3. Fig. 7 illustrates the reason why we selected this value.

From each regression curve, the threshold of a shading status is determined corresponding to the $E_{v\text{in_1m}}$ of 3000 lx. The threshold value ($E_{v\text{out}}$) for the status change of a blind from noblind to the slat angle 0° is 10,000 lx, the slat angle of 0° to 15° is 20,000 lx, and finally the slat angle 15° to 30° is 40,000 lx.

4. Results

4.1. Evaluation of vertical eye illuminance and glare indices with HDRI

In this section, E_v (vertical eye illuminance) and glare indices of the mock-up room were compared to that of the scale model. The measured period was May 2013–October 2013.

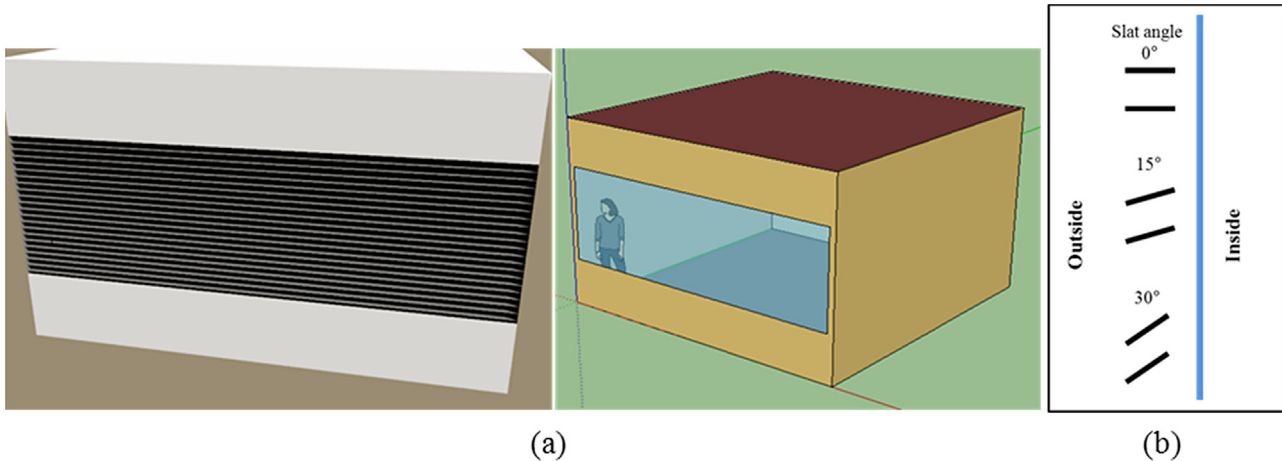


Fig. 2. (a) Test space for DIVA-for-Rhino and EnergyPlus (b) Venetian blind slat angles.

The left picture is a visual field that was taken in a mock-up room, and the right one is a visual field that was taken in a scale model, in Fig. 4. The outside view of the right picture is very similar to that of the left picture, since the scale model was located in front of the window of the mock-up room. Figs. 5 and 6 show the E_v , DGP and DGPs results by the evalglare with HDRI from the mock-up room and the scale model, compared to the measurement, during August 26–September 4, 2013. All of the E_v data is measured at a point 1 m away from the outer window of the mock-up room.

During the measurement period, a clear sky and an intermediate sky with sun are mostly observed, and E_v is measured in similar sky conditions.

In Fig. 5, distribution charts show the relationship between E_v , DGP and DGPs.

The measured vertical eye illuminance of the scale model (E_v, M, sm) is very similar to the measured vertical eye illuminance of the mock-up room (E_v, M, mr). E_v, M, sm is larger than E_v, M, mr by about 3%. The vertical eye illuminance of the mock-up room with HDRI (E_v, H, mr) is larger than E_v, M, mr by about 19%. E_v from HDRI tends to be slightly overpredicted, compared to the measurement

and errors occur in the percentages of -9% to 38%. In the scale model, E_v, H, sm is generally similar to the E_v, M, sm , and errors occur of about 9%.

The tendencies of DGP and E_v , derived from evalglare with HDRI are similar. In the mock-up room and the scale model, DGPs (calculated from E_v with HDRI) corresponds to DGP (see Fig. 6(a)–(c)).

As mentioned in Section 2.2, DGP requires some factors, such as the luminance of the source, size of the source and position index. However, it is not easy to obtain them in a real situation. On the other hand, DGPs requires only vertical eye illuminance. Therefore, if we can find the E_v corresponding to the DGPs that provokes glare, then we can use the E_v as the glare index, to evaluate the visual environment.

Fig. 7 presents the correlation between DGP_H and E_v, M of the mock-up room. As mentioned above, DGPs is closely related to DGP. Moreover, according to the relationship of E_v and DGP, we can determine the criteria for glare index, as E_v corresponds to the DGP. In this research, the E_v criterion for dynamic simulation with DIVA-for-Rhino is set to 3000 lx, and this value corresponds to a DGP of 0.4.

Table 5
Simulation layout.

Field	EnergyPlus, DIVA-for-Rhino
Simulation tool	
Weather file (from DOE)	KOR_Inchon_IWEC.epw
Test space	Size WWR Tvis Window U-factor SHGC Floor Ceiling Wall EHP (Electric Heat Pump)
Surface reflectance	5(w) × 5(d) × 3(h) [m ³] 50% 50% 1.258 0.35 20% 70% 50% COP 3.0 0.7 [ACH]
HVAC system	0.065 [person/m ²] 15 [W/person], fraction radiant 0.83, sensible heat fraction 0.61
Ventilation + infiltration	9.2 [W/m ²] 5.4 [W/m ²]
Internal gains	0.09 [m] 0.07 [m] No blind, 0°, 15°, 30° 70%
Exterior venetian blind	Work plane at 0.75 m 500 [lx] 09:00–18:00 for weekdays
Lighting level	
Schedule	

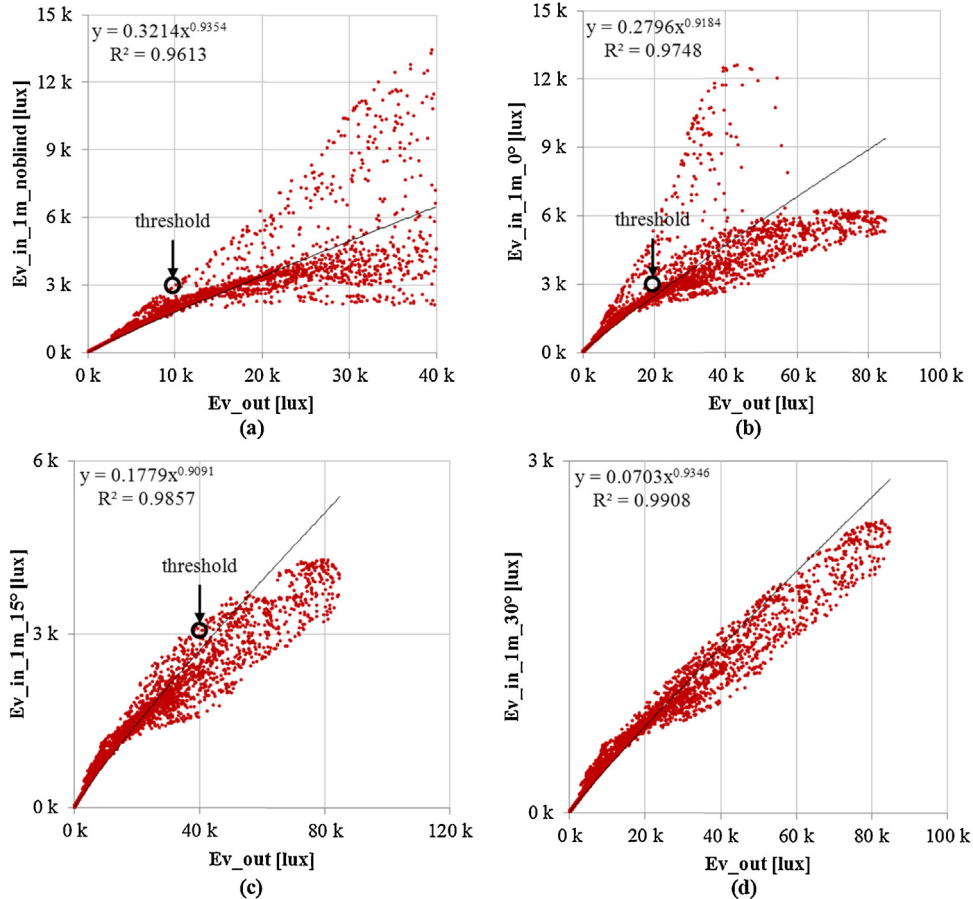


Fig. 3. Relationship between the vertical eye illuminance ($Ev.in.1m$) and the exterior vertical illuminance ($Ev.out$).

4.2. Validation of E_v from DIVA-for-Rhino

In this research, the *DIVA-for-Rhino* program was used to evaluate the E_v values, according to the changes in building orientation, and shading device. $Ev.R,mr$ is obtained by the *evalglare* with HDRI from *DIVA-for-Rhino*. To validate this program, $Ev.R,mr$ is compared to the measured E_v ($Ev.M,mr$), and *gendaylit* together with measured irradiances (direct and diffuse horizontal irradiance) were used to make the same sky condition.

In Fig. 8, the measured values of $Ev.M,mr$ are the standard values; however, $Ev.R,mr$ is overpredicted by about 12%. In

following section, the simulation was performed by *DIVA-for-Rhino*, to evaluate the visual environment, according to the orientation and venetian blind.

4.3. Dynamic simulation of visual comfort and control strategy for the venetian blind

DIVA-for-Rhino performed the dynamic simulation of DGP and E_v according to three orientations (south, east and west), and four states of the blind (no blind, slat at 0°, 15°, and 30°).

Figs. 9–11 present the annual DGP from *DIVA-for-Rhino* for the three orientations of the building, and the four static controls of



Fig. 4. HDR images of the mock-up room (left), and scale model (right) with venetian blind.

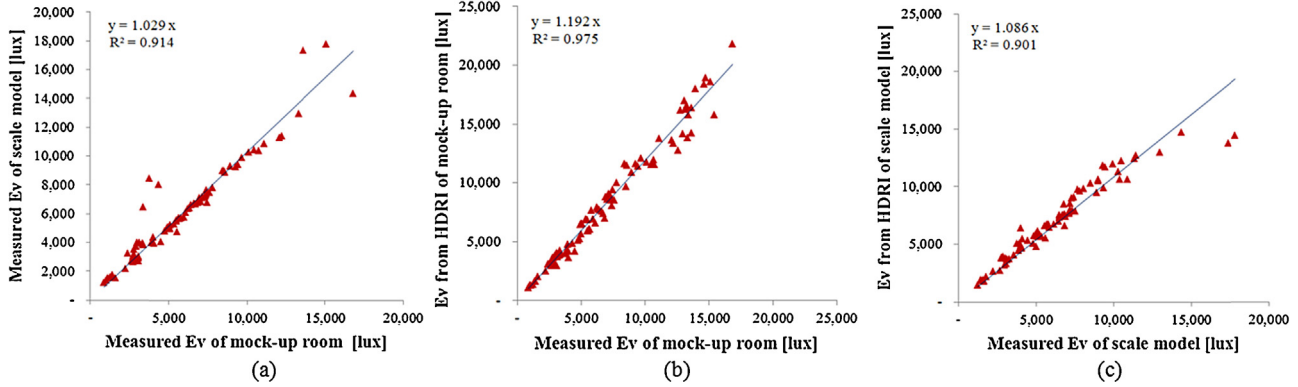


Fig. 5. Correlation between: (a) the measured E_v of the mock-up room, and the measured E_v of the scale model, (b) the measured E_v of the mock-up room, and the E_v from HDRi of the mock-up room, (c) the measured E_v and the E_v from HDRi in the scale model.

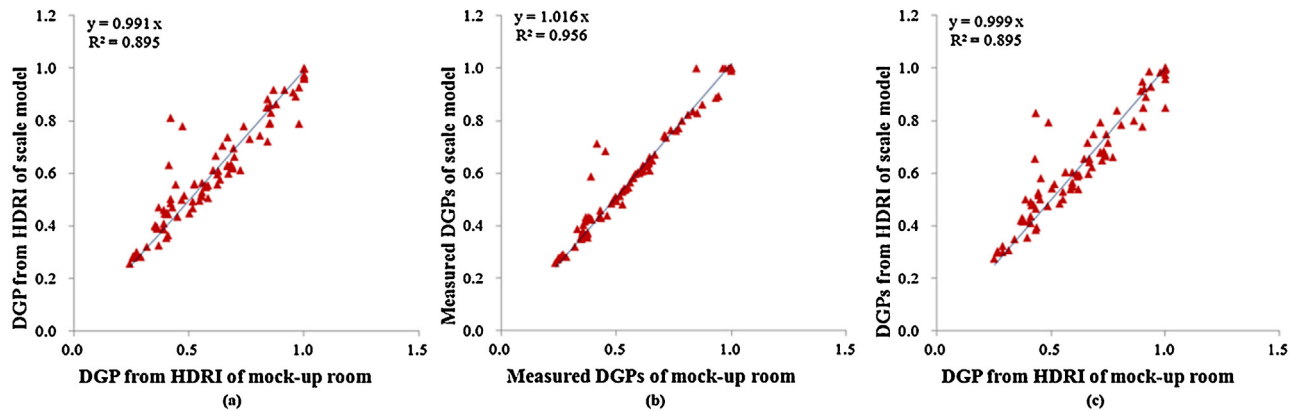


Fig. 6. Correlation between: (a) DGP from HDRi of the mock-up room and the scale model, (b) DGPs from measured E_v of the mock-up room and the scale model, and (c) DGPs from HDRI of the mock-up room and the scale model.

the venetian blind. In most cases, the glare occurs near the window; therefore the authors suppose the severe situation at 1 m away from the window, to evaluate the visual comfort.

Fig. 9 presents the annual DGP in the south façade, and 1 m away from the window. In the case of no blind, there is disturbing glare of 59% in a year; 27% for 0° slat angle; 2% for 15° slat angle, and 0.2% for 30° slat angle. Fig. 10 presents the annual DGP in the east façade.

Most of the glare occurred in the morning. In the case of no blind, there is disturbing glare of 37% in a year; 13.6% for 0° slat angle; 3.5% for 15° slat angle, and 0.8% for 30° slat angle. Fig. 11 presents the annual DGP in the west façade building. Most of the glare occurred in the afternoon. In the case of no blind, there is disturbing glare of 38.3% in a year; 15.9% for 0° slat angle; 3.3% for 15° slat angle, and 0.4% for 30° slat angle.

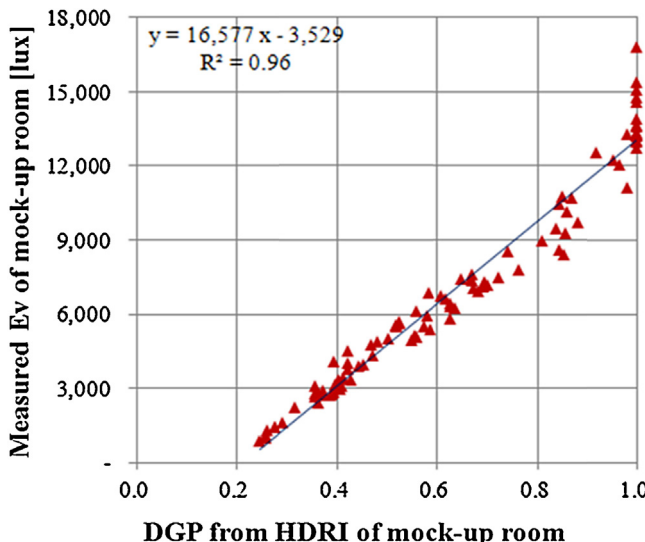


Fig. 7. Correlation between DGP_H,mr and Ev_M,mr.

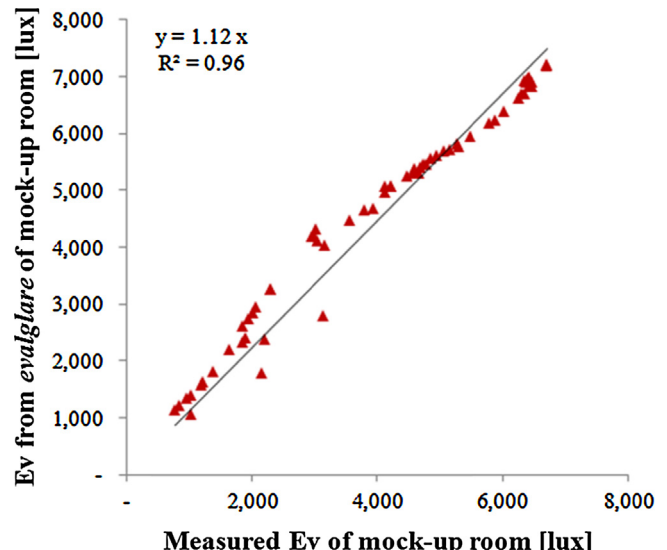


Fig. 8. Correlation between Ev_M,mr and Ev_R,mr.

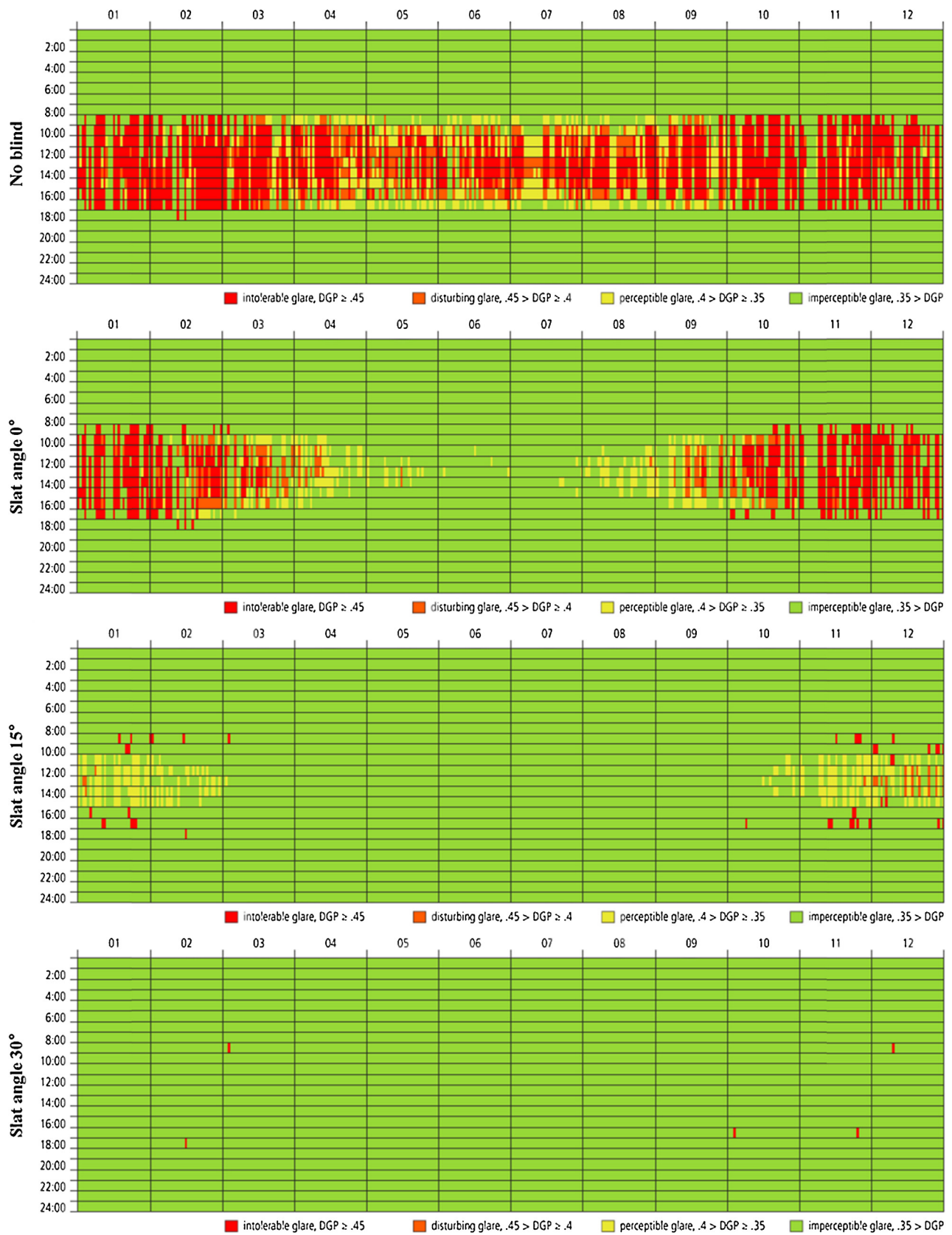


Fig. 9. Annual DGP from DIVA-for-Rhino (south façade, 1 m from the window).

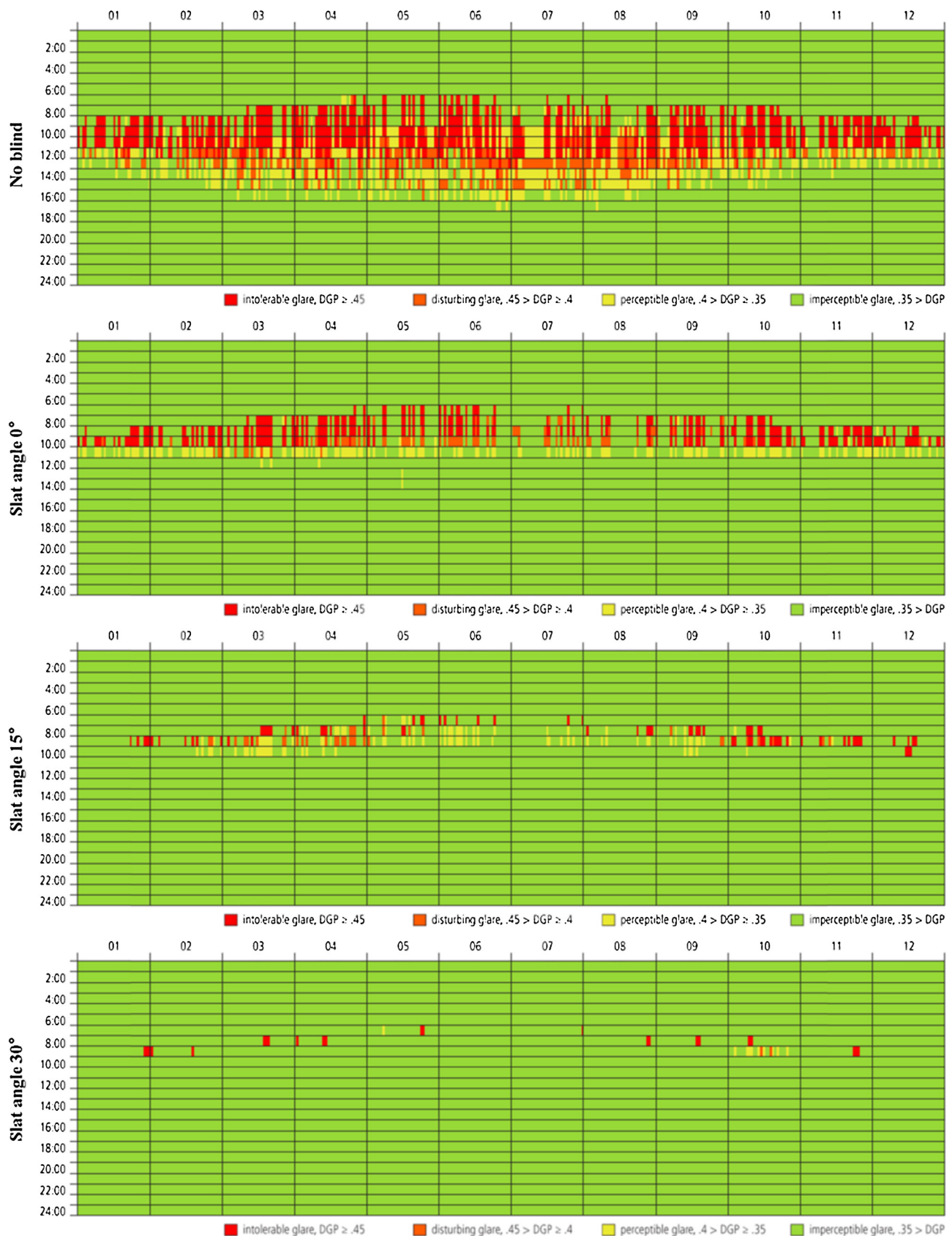


Fig. 10. Annual DGP from DIVA-for-Rhino (east façade, 1 m from the window).

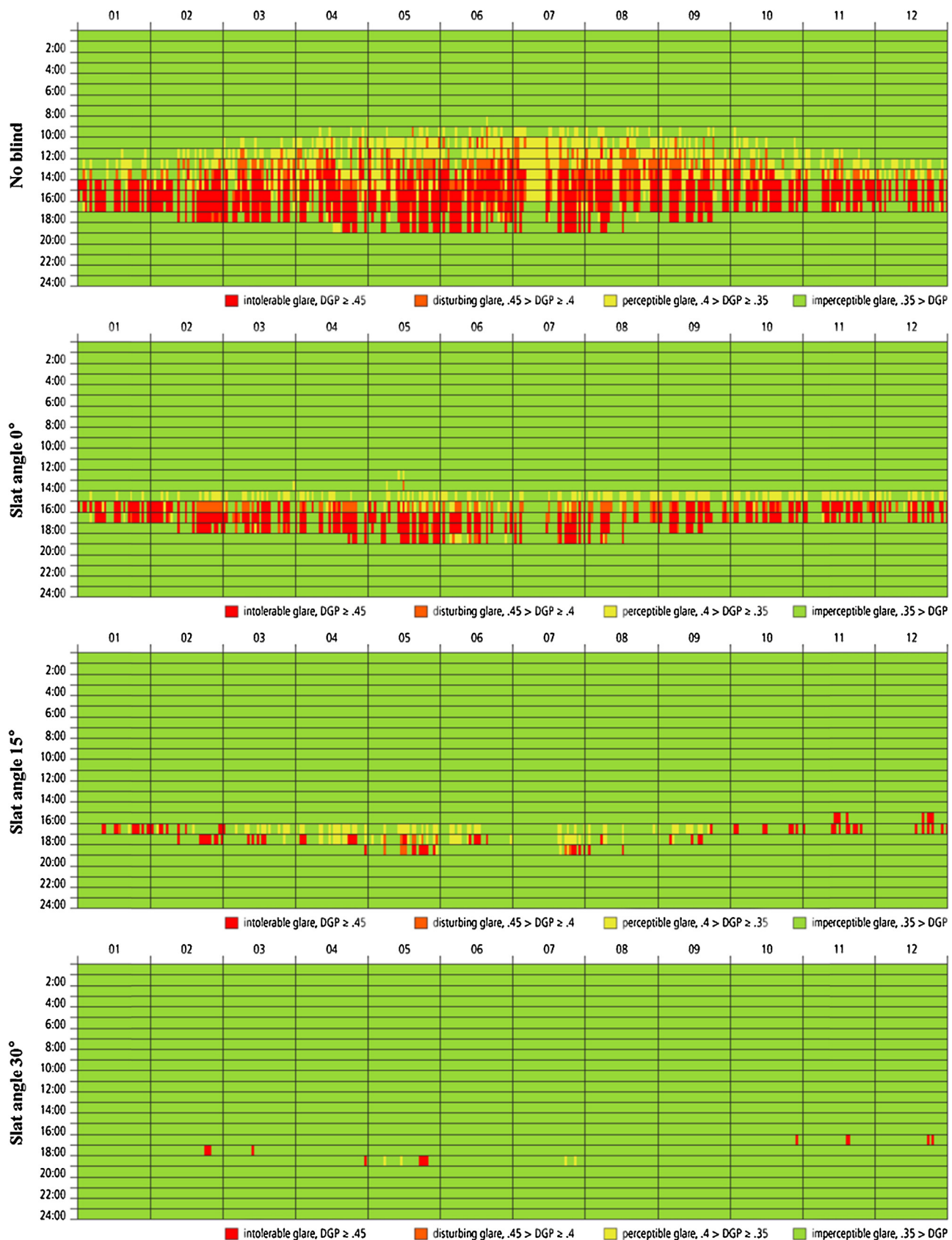


Fig. 11. Annual DGP from DIVA-for-Rhino (west façade, 1 m from the window).

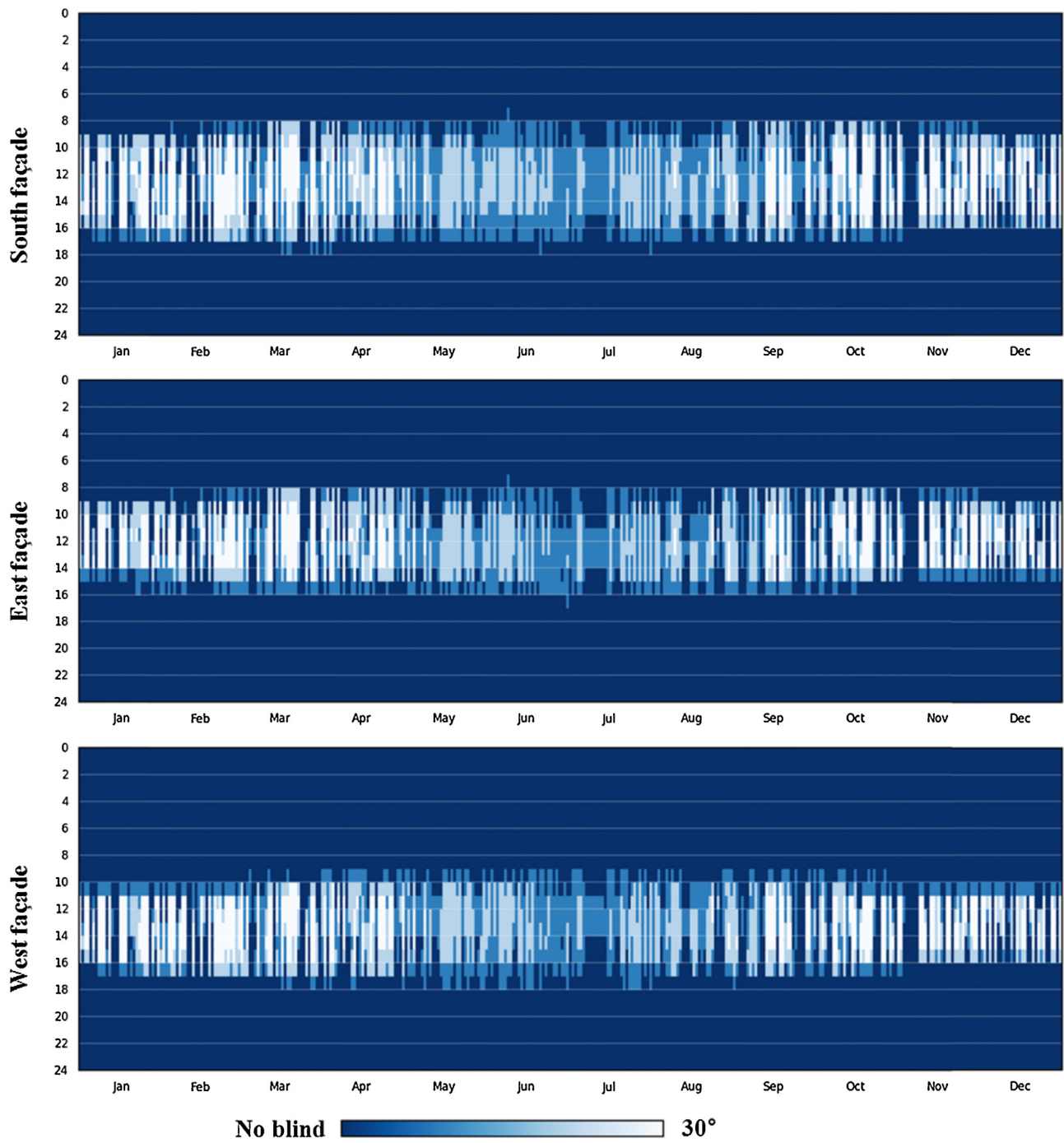


Fig. 12. Annual shading control strategies (dynamic shading).

If dynamic shading control is performed, the annual shading control strategy is as described in Fig. 12.

As described in above section, the E_v value of 3000 lx can be used for the glare index. In Fig. 12, the optimized hourly slat angles for the south, east and west façade buildings are suggested, according to the E_v value. The objective of this optimization is to prevent disturbing glare, and secure maximum daylight at the same time.

4.4. Building energy consumption by the control strategies of lighting and shading

4.4.1. Cases for the energy analysis

In this section, the results of the energy consumption with the control strategies of the lighting and shading are presented.

The cases in Table 6 for energy analysis are selected according to the building orientation and control strategy of the lighting and shading. The lighting control strategies are of two types: the on/off control, and the dimming control. The static blind control means that the venetian blind is fixed to the slat angle set by the user, and the dynamic blind control means that the blind slat is controlled automatically, to avoid glare (E_v value of less than 3000 lx). With this dynamic shading control, the slat angle of the venetian blind automatically varies from no blind to 30°.

4.4.2. Annual energy consumption by control strategies

The results of the annual energy consumption by the control strategies are presented in Figs. 13–18.

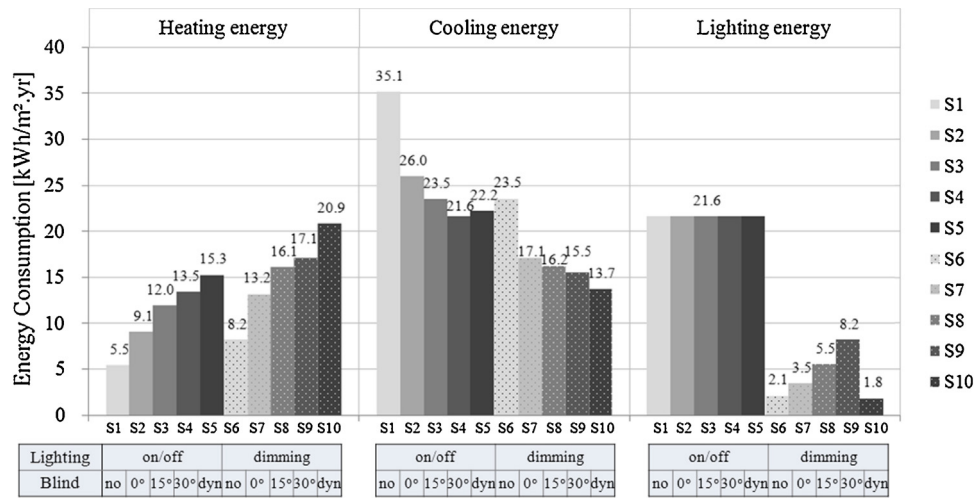


Fig. 13. Annual heating, cooling and lighting energy consumption for south-facing building.

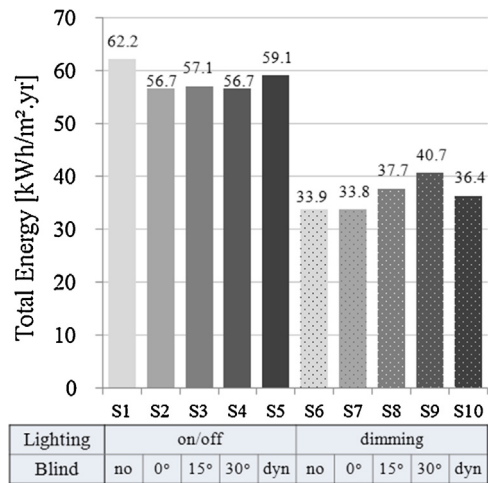


Fig. 14. Annual total energy consumption for the south-facing building.

For the south-facing building, the heating energy is increased in proportion to the angle of the venetian blind, regardless of the lighting control. The cooling energy with on/off control of the lights is decreased in inverse proportion to the angle; but the

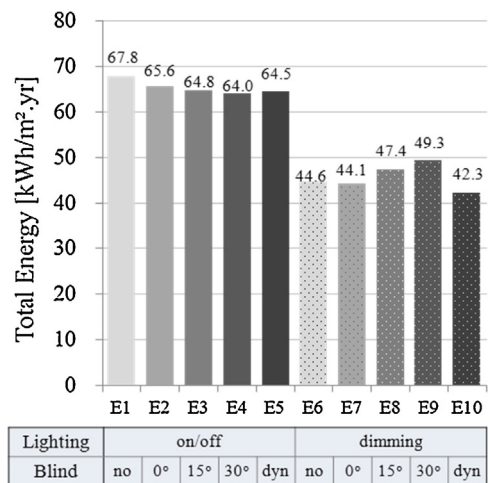


Fig. 16. Annual total energy consumption for the east-facing building.

cooling energy with dimming control of the lights does not have the same tendency. In the case of the 30° angle (S9), the radiant heat from the lights affects the increase of the cooling energy. For the dynamic shading control (S10), the heating energy has the

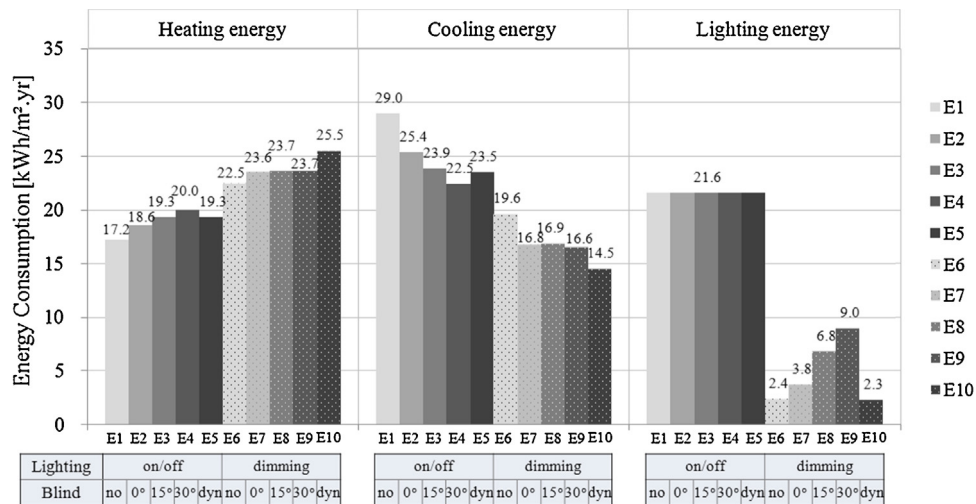


Fig. 15. Annual heating, cooling and lighting energy consumption for the east-facing building.

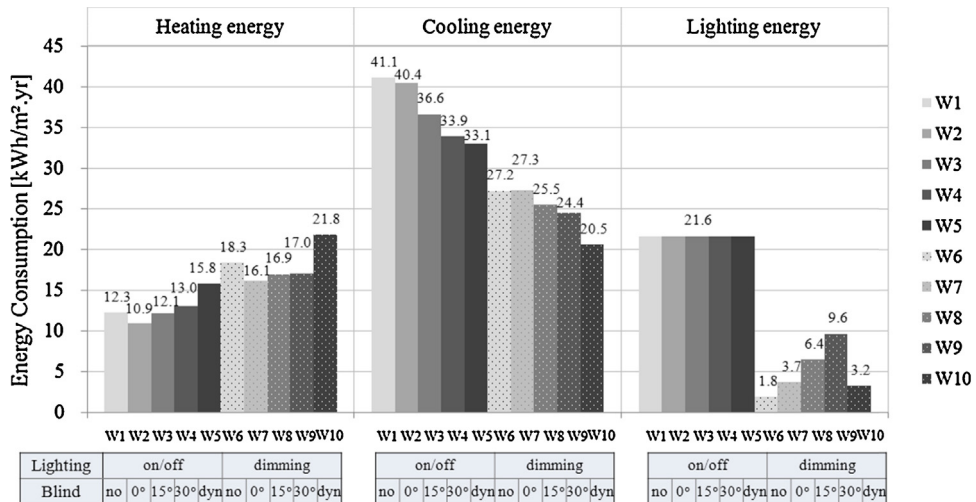


Fig. 17. Annual heating, cooling and lighting energy consumption for the west-facing building.

maximum value, and the cooling energy has the minimum value (see Fig. 13).

The total energy consumption for the south-facing building with the on/off control of the lights is decreased in inverse proportion to the slat angle (S1–S4); but with the dimming control of the lights, the total energy consumption is increased, in proportion to the slat angle (S7–S9). The total energy consumption by the dynamic shading control (S10) is bigger than the case of 0° slat angle (S7), but if we choose the control strategy of S7, glare can occur, and occupants feel discomfort. Therefore, the dynamic shading control with the dimming control of the lights is the best case (S10) (see Fig. 14).

For the east-facing building with the on/off control of the lights, the heating energy is increased in proportion to the angle of the

venetian blind (E1–E4). The cooling energy with on/off control of the lights is decreased, in inverse proportion to the angle (E1–E4); but the cooling energy with dimming control of the lights does not have the same tendency. Generally, an increase in blind slat angle affects the cooling energy to be decreased. In this case, the radiant heat from the lights affects the cooling energy; therefore, the cooling energy increased in proportion to the blind slat angle. For the dynamic shading control (E10), the heating energy has the maximum value, and the cooling energy has the minimum value (see Fig. 15).

The total energy consumption for the east-facing building with the on/off control of the lights is decreased, in inverse proportion to the slat angle (E1–E4). However, the total energy consumption is increased, in proportion to the slat angle (E5–E9), with the dimming control of the lights. The total energy consumption is the smallest, in the case of E10 (see Fig. 16).

For the west-facing building with the on/off control of the lights, the energy consumption tendency is similar to that of the south or east facing buildings. However, the cooling energy with dynamic shading (W5) does not have the same tendency as the west-facing building. The cooling energy is more affected by the lighting energy; therefore the cooling energy with dynamic shading is the smallest (W10). For the dynamic shading control (W5 and W10), the heating energy has the maximum value, and the cooling energy and the lighting energy have the minimum values (see Fig. 17).

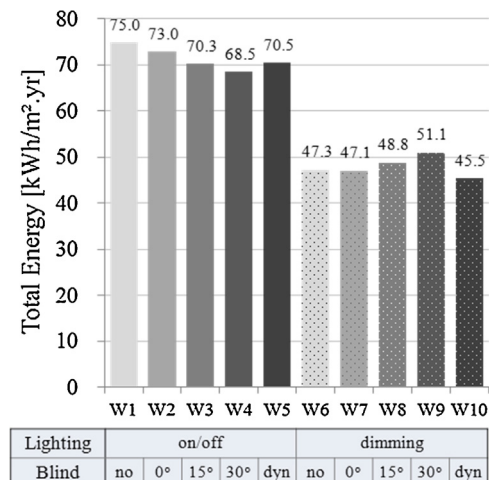


Fig. 18. Annual total energy consumption for the west-facing building.

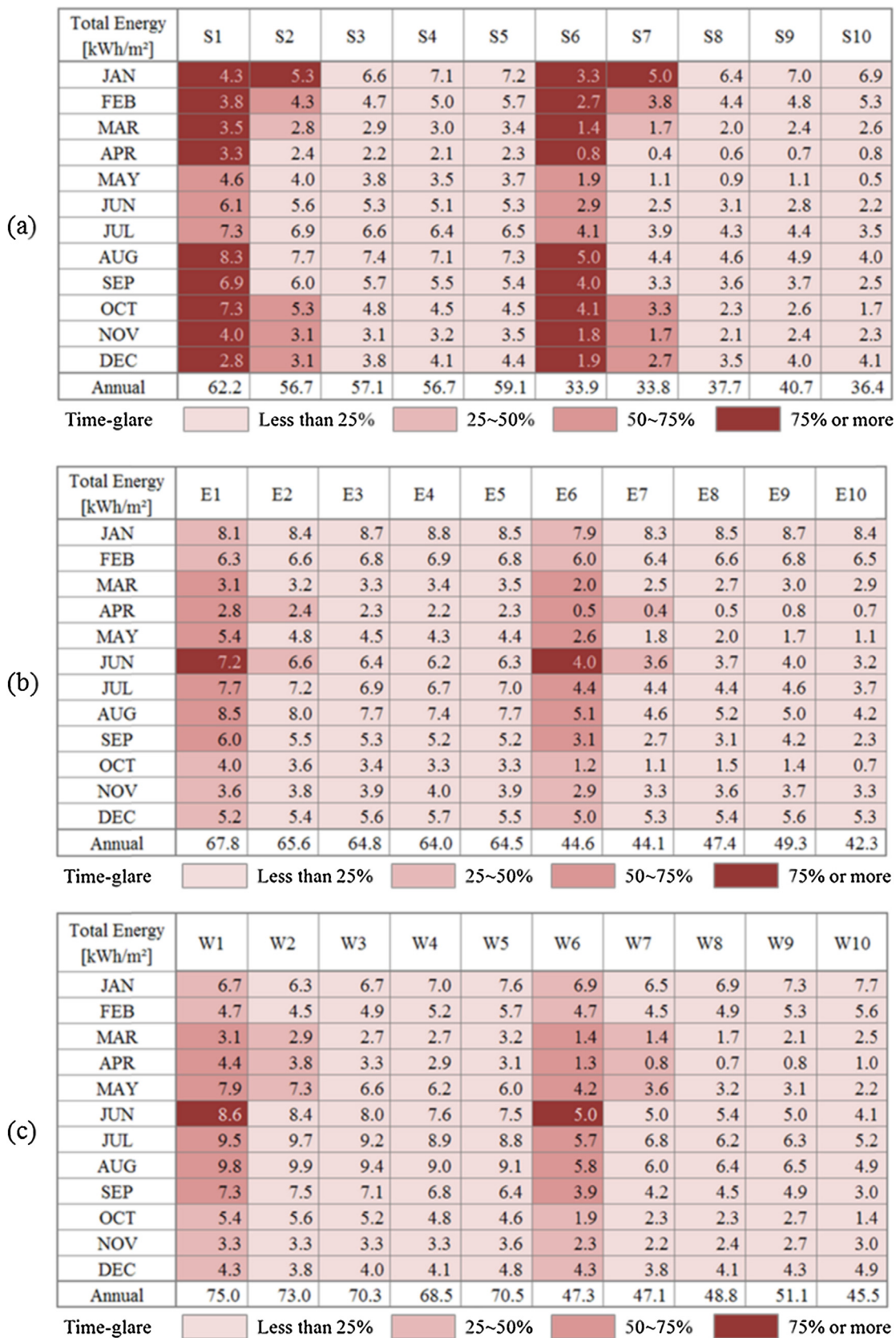


Fig. 19. Monthly total energy consumption, and the time-glare for: (a) the south-facing building, (b) the east-facing building, (c) the west facing building.

The total energy consumption for the west-facing building with the on/off control of the lights is decreased, in inverse proportion to the slat angle (W1–W4). However, with the dimming control of the lights, the total energy consumption is increased, in proportion to the slat angle (W7–W9). The total energy consumption is the smallest in the case of W10. If there is no dimming system, it is better to choose the fixed 30° slat angle (W4), to save building energy, and to avoid glare discomfort (see Fig. 18).

4.4.3. Monthly energy consumption by control strategies

In this section, the monthly energy consumptions according to the control strategies are presented. The following figures describe the monthly total energy consumption per area, and the time-glare at the same time. The cells with a very light red present the time-glare that is less than 25% of the month; 25–50% of the time-glare for the cell with the second lightest red; 50–75% for the cells with the third lightest red, and 75% or more for the cells with red. These can be used for the selection of the lighting and shading control strategies in a month, or a season.

Fig. 19 presents the monthly total energy consumption and the time-glare for the south, east and west facing buildings. For the south-facing building, if the energy consumption has a priority, the case of S6 (no blind) can be selected for the control strategy in January. However, unintended glare can exist in about 75% or more of the time. The case of S8 (15° slat angle) is suitable for the control strategy in January. If there is no need to consider the glare, the case of S1 (lights on/off and no blind) or S6 (dimmable lights and no blind) is better for the control strategy in winter (December to February). For summer (June to August), the case of S4 (30° slat angle, with the lights on/off) or S10 (dynamic shading control, with dimmable lights) is suitable for the control strategy.

For the east-facing building, if there is no need to consider the glare, the case of E1 or E6 (no blind) is suitable for the control strategy in winter (December to February). For summer (June to August), the case of E4 (30° slat angle, with the lights on/off) or E10 (dynamic shading control with dimmable lights) is suitable for the control strategy.

For the west-facing building, if there is no need to consider the glare, the case of W2 or W7 (0° slat angle) is suitable for the control strategy in winter (December to February). For summer (June to August), the case of W5 or W10 (dynamic shading control) is suitable for the control strategy.

5. Conclusions

In this research, the daylighting is considered as an important source of visual comfort and energy savings. The proper façade design, and control strategies for shading devices or electric lights can greatly help in reducing not only lighting energy use, but also HVAC energy use.

The glare index of DGP is designed to evaluate the visual environment. However, it is not easy to calculate it in a real scene. Therefore, we suggested the vertical eye illuminance (E_v) of 3000 lx as a threshold value, for the control of shading devices. This value corresponds to the DGP or the DGPs of 0.4 (means disturbing glare). The annual control strategy of the venetian blind was suggested in this research according to the E_v value of 3000 lx. We can prevent disturbing glare and secure maximum daylight by this optimized control strategy.

After applying the threshold value, the building energy consumptions are calculated. The integrated simulation method (ISM) of *EnergyPlus* and *DIVA-for-Rhino* was applied for the accurate prediction of lighting energy. The cases are set according to the 3 building orientations, the 2 lighting control strategies and the 10 blind control strategies. For all buildings, the total energy consumption with the on/off control of the lights is decreased, in inverse

proportion to the blind slat angle; but with the dimming control of the lights, the total energy consumption is increased, in proportion to the slat angle. The dynamic shading control with the dimming control of the lights is the best case for the east and the west facing buildings. For the south facing building, the case of 0° slat angle represents the smallest energy consumption, but glare can occur. The tendency of the monthly energy consumption is slightly different from that of the annual energy consumption. If there is no need to consider the glare, a slat angle of 0° or dynamic shading is better for the control strategy in winter, regardless of the building orientation. However, unintended glare can occur. In summer, the case of 30° slat angle or dynamic shading is suitable for an energy efficient and anti-glare control strategy in south facing building. The cooling energy is inversely proportional to the heating and lighting energy. If the shading is controlled to minimize the cooling load, it can affect an increase of the lighting energy. Therefore, the control strategy can differ by priority, or by season.

Acknowledgement

This research was supported by the Basic Science Research Program, through the National Research Foundation of Korea, funded by the Ministry of Education, Science and Technology (NRF-2013R1A1A2A10005456). Also, this research was supported by a Korea University Grant.

References

- [1] M.S. Alrubaih, M.F.M. Zain, M.A. Alghoul, N.L.N. Ibrahim, M.A. Shameri, O. Elayeb, Research and development on aspects of daylighting fundamentals, *Renewable and Sustainable Energy Reviews* 21 (1) (2013) 494–505.
- [2] M.B. Hirning, G.L. Isordi, I. Cowling, Discomfort glare in open plan green buildings, *Energy and Buildings* 70 (2014) 427–440.
- [3] M.B.C. Aries, J.A. Veitch, G.R. Newsham, Windows, view, and office characteristics predict physical and psychological discomfort, *Journal of Environmental Psychology* 30 (2010) 533–541.
- [4] M. Boubekri, L.L. Boyer, Effect of window size and sunlight presence on glare, *Lighting Research and Technology* 24 (2) (1992) 69–74.
- [5] P. Leather, M. Pyrgas, D. Beale, C. Lawrence, Windows in the workplace: sunlight, view, and occupational stress, *Environment and Behavior* (1998) 739–762.
- [6] C.A. Hviid, T.R. Nielsen, S. Svendsen, Simple tool to evaluate the impact of daylight on building energy consumption, *Solar Energy* 82 (2008) 787–798.
- [7] D.H.W. Li, A review of daylight illuminance determinations and energy implications, *Applied Energy* 87 (2010) 2109–2118.
- [8] M. Kartti, P.M. Erickson, T.C. Hillman, A simplified method to estimate energy savings of artificial lighting use from daylighting, *Building and Environment* 40 (2005) 747–754.
- [9] G. Yun, K. Kim, An empirical validation of lighting energy consumption using the integrated simulation method, *Energy and Buildings* 57 (1) (2013) 144–154.
- [10] R. Taylor, C. Pedersen, L. Lawrie, Simultaneous Simulation of Buildings and Mechanical Systems in Heat Balance Based Energy Analysis Programs, *BLAST Support Office*, 1993.
- [11] Lawrence Berkeley Laboratory, Los Alamos National Laboratory, DOE-2 Engineers Manual, U.S. Department of Energy, 1982.
- [12] EnergyPlus, Getting Started with EnergyPlus, Lawrence Berkeley National Laboratory, Berkeley, CA, 2010.
- [13] F.C. Winkelmann, Daylighting calculation in DOE-2, Lawrence Berkeley National Laboratory, Berkeley, CA, 1983.
- [14] F.C. Winkelmann, S. Selkowitz, Daylighting simulation in DOE-2 building energy analysis program, *Energy and Buildings* 18 (1) (1985) 271–286.
- [15] Solemma, DIVA for Rhino. Retrieved from DIVA For Rhino, Online at <http://diva4rhino.com>
- [16] R.G. Hopkinson, Glare from daylighting in buildings, *Applied Ergonomics* 3 (4) (1972) 206–215.
- [17] P. Chauvel, J.B. Collins, R. Dogniaux, Glare from windows: current views of the problem, *Lighting Research and Technology* (1982) 31–46.
- [18] J. Wienold, J. Christoffersen, Evaluation methods and development of a new glare prediction model for daylight environments with the use of CCD cameras, *Energy and Buildings* 38 (1) (2006) 743–757.
- [19] J. Suk, M. Schiler, Investigation of Evalglare software, daylight glare probability and high dynamic range imaging for daylight glare analysis, *Lighting Research and Technology* (2012) 1–14.
- [20] J. Wienold, Dynamic simulation of blind control strategies for visual comfort and energy balance analysis, *Building Simulation* (2007) 1197–1204.
- [21] J. Wienold, Evalglare Documentation v1.11, 2012.
- [22] IESNA, The IESNA Lighting Handbook, ninth ed., IESNA, 2000.

- [23] KSA, KS A 3011 Recommended Levels of Illumination, 1998.
- [24] A.J. Drummond, On the measurement of sky radiation, *Archives for Meteorology Geophysics and Bioclimatology Series B* 7 (1956) 413–436.
- [25] B.A. LeBaron, J.J. Michalsky, R. Perez, A simple procedure for correcting shadowband data for all sky conditions, *Solar Energy* 44 (5) (1990) 249–256.
- [26] F.J. Batiles, F.J. Olmo, L. Alados-Arboledas, On shadowband correction methods for diffuse irradiance measurements, *Solar Energy* 54 (2) (1995) 105–114.
- [27] T. Muneer, X. Zhang, A new method for correcting shadow band diffuse irradiance data, *Solar Energy Engineering* 124 (1) (2002) 34–43.
- [28] G. Ward, Photosphere, Anywhere Software, <http://www.anyhere.com/>
- [29] Cannon, EOS 5D Mark II Instruction Manual.
- [30] ASHRAE, *ASHRAE Handbook Fundamentals*, ASHRAE, 2009.